

A complete set of novel 2D correlation NMR experiments based on heteronuclear J-cross polarization

Teodor Parella

Servei de Ressonància Magnètica Nuclear, Universitat Autònoma de Barcelona, E-08193, Bellaterra, Barcelona, Spain

Received 16 September 2003; Accepted 8 December 2003

Key words: coherence-order selective, heteronuclear correlation, heteronuclear cross-polarization, sensitivity-enhancement, spin-state-selective excitation, TROSY

Abstract

A suite of multiple-purpose sensitivity-enhanced 2D correlation NMR experiments based on heteronuclear J-cross polarization (HCP) techniques are introduced for isotropic liquid samples. Several pulse sequences using an adaptable heteronuclear TOCSY mixing building block are proposed for different types of effective coherence-order-selective (COS) heteronuclear coherence-transfer mechanisms. They are based on the anisotropic behaviour of the involved HCP process that is easily described and analysed in terms of cartesian product-operator formalism. A number of different versions are given for in-phase to in-phase (II-COS: $S^- \rightarrow I^-$), in-phase to anti-phase (IA-COS: $S^- \rightarrow 2I^-S_z$), in-phase to spin-state-selective (IS³-COS: $S^- \rightarrow 2I^-S^{\alpha/\beta}$), anti-phase to in-phase (AI-COS: $2I_zS^- \rightarrow I^-$), anti-phase to anti-phase (AA-COS: $2I_zS^- \rightarrow 2I^-S_z$), anti-phase to spin-state-selective (AS³-COS: $2I_zS^- \rightarrow 2I^-S^{\alpha/\beta}$) and spin-state-selective to spin-state-selective (S³S³-COS: $2I^{\alpha/\beta}S^- \rightarrow 2I^-S^{\alpha/\beta}$) coherence transfers. The combination of the echo/anti-echo approach, heteronuclear gradient echoes and the preservation of equivalent pathways (PEP) methodology affords a general approach to obtain sensitivity-enhanced pure-absorption 2D spectra that can be used as interesting alternatives to conventional pulse-interrupted free-precession INEPT-based pulse schemes, such as HSQC-type and TROSY-type experiments.

Abbreviations: COS – Coherence Order Selective; PFG – Pulsed Field Gradients; HCP – Heteronuclear Cross Polarization; PEP – Preservation of Equivalent Pathways; S³ – Spin State Selective.

Introduction

The HSQC experiment (Bodenhausen et al., 1980) is probably the most important pulse sequence in bio-molecular NMR. During the last years, the growing number of successful modifications introduced in the HSQC pulse sequence has taken great relevance because they can also be incorporated into many multidimensional NMR experiments based on the same principles. Nowadays, the most accepted version of the ¹H-X HSQC correlation experiment is the sensitivity-enhanced HSQC-PEP pulse scheme (Kay et al., 1992) that presents the following fea-

tures: i) Coherence selection by pulsed-field gradients (PFGs), ii) maximum sensitivity and optimised resolution obtained by combination of the echo/anti-echo approach and PEP methodology, iii) effective solvent suppression achieved by the exclusive effect of PFGs and, optionally, reinforced by applying the water flip-back technique, iv) wide use on different pairs of active NMR nuclei, v) broad application on natural-abundance compounds and also labelled biomolecules, and vi) great flexibility to accommodate new NMR elements.

The design of modified HSQC experiments that selectively manipulate the α or/and β spin state in some way has emerged as an interesting concept in multidimensional NMR spectroscopy. For instance, the

*To whom correspondence should be addressed. E-mail: teo@rnm3.uab.es

old E. COSY principle (Griesinger et al., 1985) is an important and extended tool widely applied for the determination of homo- and heteronuclear coupling constants in labelled bio-molecules. In the resulting E. COSY spectra, the relative displacement between cross-peaks generated from the α and β spin state is used to determine the sign and the magnitude of even tiny coupling constant values. Recently, it has appeared a great number of related HSQC versions that allow the exclusive selection of the α or β spin states in separate 2D spectra. A simple example is the HSQC- α/β experiment (Sorensen et al., 1997, 1999; Andersson et al., 1998b; Kozminski, 1999) in which the second retro-INEPT pulse train of the regular HSQC-PEP experiment (Palmer et al., 1991) is reduced to a single 90° X pulse. This reduced PEP building block selects two different coherences, one as in-phase multiplet and the second showing an anti-phase pattern. The simultaneous addition or subtraction of these coherences before acquisition affords the exclusive selection of a single α or β component, respectively, whereas the maximum attainable sensitivity is retained. This experiment affords w_2 -coupled spin-state-edited ^1H -X 2D correlation spectra in which only one of the two multiplet signals is present and, therefore, the number of cross-peaks remains unaffected when compared to conventional 2D spectra. Spin-state-selection (S^3) can also be achieved during the indirect evolution t_1 period, resulting a w_1 -coupled spin-state-edited ^1H -X correlation experiment, also referred as α/β -HSQC or IPAP experiment (Ottiger et al., 1998; Andersson et al., 1998b). The main advantage of this experiment is that, sometimes, transverse relaxation during the indirect X dimension is not as critical as in the observed ^1H dimension for large biomolecules. Both S^3 approaches can also be combined in a single α/β -HSQC- α/β experiment, where the popular TROSY experiment is the best example (Pervushin et al., 1997; Meissner et al., 1998; Schulte-Herbrüggen and Sorensen, 2000; Andersson et al., 1998a,b; Czisch and Boelens, 1998), in which the resulting w_1 - w_2 -coupled doubly- S^3 -edited HSQC spectrum only displays, for an IS spin system, one of the four expected cross-peaks. All these edited NMR experiments are actually widely used to measure scalar and residual dipolar coupling constants and also configure the fundamentals of modern NMR methodologies dedicated to the structural and dynamic studies on large bio-molecules in higher magnetic fields.

In this work, a suite of powerful and very versatile NMR correlation experiments is presented as attract-

ive alternatives to traditional HSQC experiments. The main feature of the suggested pulse sequences is the use of heteronuclear cross polarization (HCP) to transfer magnetization from X to ^1H and/or from ^1H to X instead of the habitual INEPT-based pulse trains. In fact, the idea to use HCP in isotropic liquids is old and a number of different works already described its theoretical aspects (Bertrand et al., 1978; Muller and Ernst, 1979; Chingas et al., 1981; Zuiderweg, 1990; Ernst et al., 1991; Levitt, 1991; Glaser and Quant, 1996) and several applications have been reported for proteins (Majumdar and Zuiderweg, 1995; Shirakawa et al., 1995; Richardson et al., 1995; Wang and Zuiderweg, 1995; Zuiderweg et al., 1996) and nucleic acids (Wijmenga et al., 1995; Simorre et al., 1995; Sklenar et al., 1996). However, in the last decade HMQC-like and HSQC-like experiments have been accepted as the standard pulse schemes to work on small molecules and also on large unlabeled and labeled bio-molecules. In contrast to these free-precession ^1H -X correlation experiments, HCP experiments relies on the application of two magnetic fields synchronously applied to both ^1H (denoted as I spin) and X (denoted as S spin) nuclei (with intensities $\omega_{1I} = \gamma^I B_1^I / 2\pi$ and $\omega_{1S} = \gamma^S B_1^S / 2\pi$, respectively) and maximum heteronuclear coherence transfer is achieved when the so-called Hartmann-Hahn condition is fulfilled (Hartmann and Hahn, 1962).

As predicted theoretically, the HCP-based experiments described herein offer maximum sensitivity ratios due to the selection and combination of two different observable magnetizations. The anisotropy of the heteronuclear coherence transfer involving HCP mixing processes is clearly demonstrated by the strong dependence of the transfer mechanism with respect to the relative phase between the input magnetization and the HCP mixing sequence (T. Parella, submitted). A series of closely-related NMR pulse schemes have been designed that allow a simple and specific manipulation of distinct coherences available before and after the mixing HCP process, making them very interesting for many different applications. It is clearly shown here that, for a given IS spin system, in-phase or anti-phase S magnetization can be specifically transferred with high efficiency to in-phase and/or anti-phase I magnetization by a suitable rearrangement of the proposed mixing HCP process. Various examples for in-phase to in-phase (II-COS: $S^- \rightarrow I^-$), in-phase to anti-phase (IA-COS: $S^- \rightarrow 2I^- S_z$), in-phase to spin-state-selective (IS^3 -COS: $S^- \rightarrow 2I^- S^{\alpha/\beta}$), anti-phase to in-phase (AI-COS: $2I_z S^- \rightarrow I^-$), anti-phase

to anti-phase (AA-COS: $2I_z S^- \rightarrow 2I^- S_z$), anti-phase to spin-state-selective (AS³-COS: $2I_z S^- \rightarrow 2I^- S^{\alpha/\beta}$) and spin-state-selective to spin-state-selective (S³S³-COS: $2I^{\alpha/\beta} S^- \rightarrow 2I^- S^{\alpha/\beta}$) coherence transfers are provided. Remarkable aspects such as excellent results in terms of sensitivity, good tolerance to rf inhomogeneities (Levitt, 1991), a better behaviour under relaxation and chemical exchange phenomena (Levitt, 1991; Krishnan and Rance, 1995; Zangger and Armitage, 1998) and the high versatility available from the proposed general pulse schemes using minor modifications can be potential reasons for the choice of these HCP experiments instead of conventional HSQC counterparts when required.

Results and discussion

Theory

In order to understand the new developed NMR pulse sequences using a simple product-operator formalism description, the effect of the HCP mixing sequence on different one-spin and two-spin cartesian operators must be evaluated (Sorensen, 1983). Through this work it will be assumed that HCP is always executed as simultaneous DIPSI-2 mixing sequences applied from the y-axis (denoted as HCP(y)) in both independent I and S channels. Under such conditions, the effective coupling term of the active Hamiltonian during the HCP(y) process is described as

$$H^{eff} = \pi J_{IS}^{eff} (2I_z S_z + 2I_x S_x). \quad (1)$$

In heteronuclear experiments, the effective coupling constant is usually given by $J_{IS}^{eff} = J_{IS}/2$ (Glaser and Quant, 1996). The bilinear cartesian product operators $2I_z S_z$ and $2I_x S_x$ mutually commute and the evolution of the density operator may be easily calculated in two consecutive (and in arbitrary order) steps:

$$\sigma(0) \xrightarrow{\pi J_{IS}\tau(I_x S_x)} \xrightarrow{\pi J_{IS}\tau(I_z S_z)} \sigma(t). \quad (2)$$

For an heteronuclear IS spin system, the following general transformations can be derived starting from different $\sigma(0)$ spin states described as in-phase S magnetization components. As shown, a different modulated transfer mechanism occurs depending of

the relative phase between the input S magnetization and the HCP process:

$$S_y \xrightarrow{HCP_y} \frac{1 + \cos(\pi J_{IS}\tau)}{2} S_y + \frac{1 - \cos(\pi J_{IS}\tau)}{2} I_y + (2I_x S_z - 2I_z S_x) \frac{\sin(\pi J_{IS}\tau)}{2}, \quad (3a)$$

$$S_x \xrightarrow{HCP_y} S_x \cos\left(\frac{\pi J_{IS}\tau}{2}\right) + 2S_y I_z \sin\left(\frac{\pi J_{IS}\tau}{2}\right), \quad (3b)$$

$$S_z \xrightarrow{HCP_y} S_z \cos\left(\frac{\pi J_{IS}\tau}{2}\right) - 2S_y I_x \sin\left(\frac{\pi J_{IS}\tau}{2}\right). \quad (3c)$$

An important conclusion of these expressions is that the efficiency of polarization transfer critically depends on the duration of the mixing HCP period. Thus, maximum in-phase to in-phase IS heteronuclear transfer is achieved when the duration of the mixing HCP process, τ , is adjusted to $1/J_{IS}$ and only if the input magnetization has the same relative phase as the HCP sequence.

$$S_y \xrightarrow{HCP_y(\tau=1/J)} I_y. \quad (4a)$$

However, HCP can be considered an anisotropic process and, therefore, another very important consequence emerges from the above Equations 3b and 3c: After an HCP(y) process of duration $1/J_{IS}$, the perpendicular S_x and S_z magnetization components are fully converted to anti-phase and multiple-quantum magnetization, respectively, as follows:

$$S_x \xrightarrow{HCP_y(\tau=1/J)} 2S_y I_z, \quad (4b)$$

$$S_z \xrightarrow{HCP_y(\tau=1/J)} -2S_y I_x. \quad (4c)$$

By analogy, the reverse I to S heteronuclear transfer during an HCP(y) mixing process optimised to $1/J_{IS}$ can be summarized by the following relations:

$$I_y \xrightarrow{HCP_y(\tau=1/J)} S_y, \quad (5a)$$

$$I_x \xrightarrow{HCP_y(\tau=1/J)} 2I_y S_z, \quad (5b)$$

$$I_z \xrightarrow{HCP_y(\tau=1/J)} -2I_y S_x. \quad (5c)$$

Expanding this analysis on all possible two-spin IS product-operators present before the HCP(y) mixing sequence, the next general transformations are obtained:

$$2I_z S_z \xrightarrow{HCP_y} 2I_z S_z, \quad (6a)$$

$$2I_z S_x \xrightarrow{HCP_y} [1 + \cos(\pi J_{IS}\tau)] I_x S_x + [1 - \cos(\pi J_{IS}\tau)] I_x S_z + (S_y - I_y) \frac{\sin(\pi J_{IS}\tau)}{2}, \quad (6b)$$

$$2I_z S_y \xrightarrow{HCP_y} 2I_z S_y \cos\left(\frac{\pi J_{IS}\tau}{2}\right) - S_x \sin\left(\frac{\pi J_{IS}\tau}{2}\right), \quad (6c)$$

$$2I_y S_z \xrightarrow{HCP_y} 2I_y S_z \cos\left(\frac{\pi J_{IS}\tau}{2}\right) - I_x \sin\left(\frac{\pi J_{IS}\tau}{2}\right), \quad (6d)$$

$$2I_y S_x \xrightarrow{HCP_y} 2I_y S_x \cos\left(\frac{\pi J_{IS}\tau}{2}\right) + I_z \sin\left(\frac{\pi J_{IS}\tau}{2}\right), \quad (6e)$$

$$2I_y S_y \xrightarrow{HCP_y} 2I_y S_y, \quad (6f)$$

$$2I_x S_z \xrightarrow{HCP_y} [1 + \cos(\pi J_{IS}\tau)] I_x S_z + [1 - \cos(\pi J_{IS}\tau)] S_x I_z + (I_y - S_y) \frac{\sin(\pi J_{IS}\tau)}{2}, \quad (6g)$$

$$2I_x S_x \xrightarrow{HCP_y} 2I_x S_x, \quad (6h)$$

$$2I_x S_y \xrightarrow{HCP_y} 2I_x S_y \cos\left(\frac{\pi J_{IS}\tau}{2}\right) + S_z \sin\left(\frac{\pi J_{IS}\tau}{2}\right). \quad (6i)$$

After an optimised $\tau = 1/J_{IS}$ mixing period, the optimum transfer for each transformation described in [6a-6i] can be simplified to:

$$2I_z S_z \xrightarrow{HCP_y(\tau=1/J)} 2I_z S_z, \quad (7a)$$

$$2I_z S_x \xrightarrow{HCP_y(\tau=1/J)} 2I_x S_z, \quad (7b)$$

$$2I_z S_y \xrightarrow{HCP_y(\tau=1/J)} -S_x, \quad (7c)$$

$$2I_y S_z \xrightarrow{HCP_y(\tau=1/J)} -I_x, \quad (7d)$$

$$2I_y S_x \xrightarrow{HCP_y(\tau=1/J)} I_z, \quad (7e)$$

$$2I_y S_y \xrightarrow{HCP_y(\tau=1/J)} 2I_y S_y, \quad (7f)$$

$$2I_x S_z \xrightarrow{HCP_y(\tau=1/J)} 2I_z S_x, \quad (7g)$$

$$2I_x S_x \xrightarrow{HCP_y(\tau=1/J)} 2I_x S_x, \quad (7h)$$

$$2I_x S_y \xrightarrow{HCP_y(\tau=1/J)} S_z. \quad (7i)$$

The transfer efficiencies for other $I_n S$ ($n > 1$) spin systems under the effect of HCP(y) have not been derived here. However, on the contrary that happens in IS spin systems, the reported optimal in-phase transfer under related planar TOCSY contributions are $1/\sqrt{2}J_{IS}$ and $0.6249/J_{IS}$ for $I_2 S$ and $I_3 S$ groups, respectively (Schleucher et al., 1994), and similar results have been obtained for II-COS experiments (Sattler et al., 1995b).

For the sake of completeness, the following complementary formulae are given. The linear combination of cartesian I_x and I_y operators defines the raising (I^+) and lowering (I^-) shift operators, which are highly useful to describe coherence-order gradient-selected NMR experiments.

$$I^+ = I_x + iI_y, \quad (8a)$$

$$I^- = I_x - iI_y. \quad (8b)$$

On the other hand, particular spin-states are well characterized using polarization operators, I^α and I^β , which can be defined as

$$I^\alpha = \frac{1}{2}(\mathbf{1} + 2I_z), \quad (8c)$$

$$I^\beta = \frac{1}{2}(\mathbf{1} - 2I_z), \quad (8d)$$

with $\mathbf{1}$ being the unity operator. Thus, taking as a reference Equations 8a-d, heteronuclear S^3 states can

be specified as sum or subtraction of in-phase and anti-phase states:

$$2I^\alpha S^- = S^- + 2I_z S^-, \quad (8e)$$

$$2I^\beta S^- = S^- - 2I_z S^-. \quad (8f)$$

From now on, all proposed NMR pulse sequences displayed in Figures 2 and 3 will be analysed by choosing the gradient coherence selection of the echo data (for instance, $S^- \rightarrow I^-$ or $2I_z S^- \rightarrow I^-$). In practice, the echo/anti-echo procedure is always applied in which the anti-echo data (for instance, $S^+ \rightarrow I^-$ or $2I_z S^+ \rightarrow I^-$) are recorded in alternate scans, by inverting the refocusing G2 gradient and the phase of some involved 90° pulse, and later on echo and anti-echo data are stored separately (Schleucher et al., 1993):

First transient (echo):

$$\exp(-i\Omega_S t_1) \exp(-i\Omega_I t_2), \quad (9a)$$

Second transient (anti-echo):

$$\exp(i\Omega_S t_1) \exp(-i\Omega_I t_2). \quad (9b)$$

In the data processing step, these phase-modulated signals are conveniently added and subtracted to afford two different amplitude modulated data according to:

$$\text{Data A (addition): } \cos(\Omega_S t_1) \exp(-i\Omega_I t_2), \quad (9c)$$

$$\text{Data B (subtraction + } 90^\circ \text{ phase correction in } t_2 \text{):}$$

$$\sin(\Omega_S t_1) \exp(-i\Omega_I t_2). \quad (9d)$$

And finally, Fourier transformation of these signals results in spectra showing pure phases and sensitivity-enhancement. In the following description, no more details will be given of this acquisition/processing procedure, which is usually implemented as a routine protocol in the software package that comes with commercial spectrometers.

NMR experiments

INEPT-INEPT experiments

Figure 1A shows the general pulse scheme of a coherence-order-selective (COS) coherence-transfer 2D correlation experiment employing pulsed field gradients for coherence selection. Basically, it contains four well-defined steps. First, a preparation

period in which ^1H to X polarization transfer is usually accomplished to generate some type of transverse X magnetization. The evolution period consists of a variable t_1 delay in which chemical shift is allowed to evolve whereas heteronuclear coupling constants are usually refocused by the effect of the central 180° ^1H pulse. In addition, during this period a gradient spin-echo block is introduced to dephase transverse X magnetization. This X magnetization is transferred back to ^1H via the mixing process and, before acquisition, a proton gradient spin-echo period refocuses only the selected magnetization that is detected with optional heteronuclear decoupling.

Because coherence selection is performed by PFGs implemented during the indirectly detected evolution t_1 period, F1-frequency discrimination is achieved in a single scan. However, two main drawbacks arise of such an approach. First, only one of the two possible coherence transfer pathways (echo or anti-echo) is selected and, therefore, a half of the available signal is discarded. Secondly, phase-modulated data is recorded and magnitude-mode representation of the resulting spectrum is required. This approach is only useful for applications where sensitivity and resolution are not mandatory. A simple strategy to obtain phase-sensitive data without need to modify the original pulse sequence is the application of the echo/anti-echo methodology described above. Although this approach in its basic form also suffers of a sensitivity loss of $\sqrt{2}$ for IS spin systems, increased sensitivity factors for all $I_n\text{S}$ spin systems can be achieved when it is combined with the PEP methodology (Kay et al., 1992; Schleucher et al., 1994; Sattler et al., 1995), in where two orthogonal and independent magnetizations are recovered at the end of the pulse sequence. For a successful implementation of this PEP methodology, effective mixing processes must be carefully designed that convert this second orthogonal component in observable magnetization.

Table 1 represents the most commonly HSQC-type experiments, that they will be defined as INEPT-INEPT correlation experiments, in where the initial preparation period is a ^1H -to-X INEPT pulse train that generates anti-phase X magnetization:

$$I_z \xrightarrow{90_x^I} -I_y \xrightarrow{\Delta - 180_x^I(S) - \Delta} 2I_x S_z \xrightarrow[90_x^S]{90_y^I} 2I_z S_y. \quad (10)$$

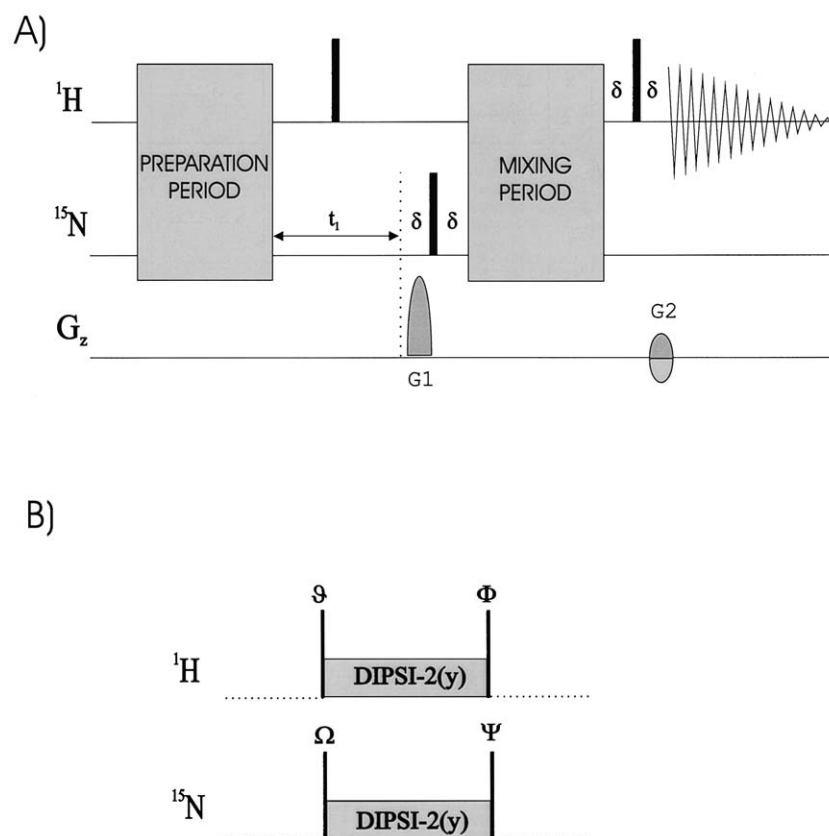
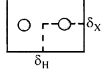
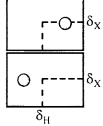
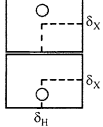
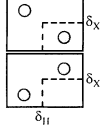
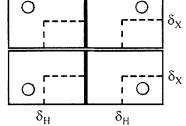


Figure 1. (A) Schematic pulse sequence scheme of a gradient-selected sensitivity-enhanced proton-detected 2D correlation experiment. The preparation period can be an INEPT, 90° (X) or an HCP-based building block, and the mixing period can be an INEPT-type or an HCP building block. (B) Universal mixing period based on heteronuclear J-cross polarization. See text for discussion about the role and the effects of the 90° (I,S) pulses applied before and after the DIPSI-2 pulse scheme and their relative Φ , Ω , ϑ and Ψ phases. Some examples and more details are given in Figures 2–3.

All 2D INEPT-INEPT correlation experiments can be classified as a function of the magnetization available during the t_1 and t_2 periods. Thus, the conventional sensitivity-enhanced HSQC-PEP experiment can be defined as an *anti-phase to in-phase*, AI-COS, experiment in which the mixing process is a double retro-INEPT building block and due to its in-phase coupling nature, it is usually recorded under heteronuclear decoupling in both dimensions. Other several related AI-COS pulse sequences have been proposed and extensively evaluated in terms of transfer efficiency for different I_nS spin systems (Schleucher et al., 1994; Sattler et al., 1995; Untidt et al., 1998). On the other hand, the modified HSQC- α/β experiment (Sorensen et al., 1997, 1999; Andersson, 1998b; Kozminski, 1999) is an *anti-phase to spin-state-selective*, AS^3 -COS, experiment only working properly for IS spin systems. In this case, the mixing period is a reduced version of the double retro-

INEPT building block. Related AS^3 -COS experiments have also been described for optimum transfer and multiplet pattern simplification in I_2S and I_3S spin systems (Sattler et al., 1996; Untidt et al., 1998, 1999). The α/β -HSQC experiment, also known as the IPAP-HSQC experiment (Ottiger et al., 1998; Andersson et al., 1998b), should be a *spin-state-selective to in-phase*, S^3I -COS experiment that afford spin-edited F1-coupled HSQC spectra. Following this same syntax, E. COSY-type and TROSY-type pulse sequences are two well-know examples of *spin-state-selective to spin-state-selective*, S^3S^3 -COS, experiments in which spin editing is performed in both dimensions. The different coupling topology obtained in all these experiments for a IS spin systems (see last column in Table 1) will be equally applicable to the proposed HCP experiments.

Table 1. General description of the most important COS 2D INEPT-INEPT NMR pulse sequences as a function of the involved coherence transfer mechanisms

Coherence-order transfer pathway	Type of transfer mechanism	NMR experiment	Coupling topology
$2S^- I_z \rightarrow I^-$	AI-COS	HSQC-PEP	
$2S^- I_z \rightarrow 2S^\alpha I^-$ $2S^- I_z \rightarrow 2S^\beta I^-$	AS ³ -COS	HSQC- α/β	
$2S^- I^\alpha \rightarrow I^-$ $2S^- I^\beta \rightarrow I^-$	S ³ I-COS	α/β -HSQC	
$2S^- I^\alpha \rightarrow 2S^\alpha I^-$ & $2S^- I^\beta \rightarrow 2S^\beta I^-$ & $2S^- I^\alpha \rightarrow 2S^\beta I^-$ & $2S^- I^\beta \rightarrow 2S^\alpha I^-$	S ³ S ³ -COS	α/β -HSQC- α/β (E. COSY-type)	
$2S^- I^\alpha \rightarrow 2S^\alpha I^-$ $2S^- I^\alpha \rightarrow 2S^\beta I^-$ $2S^- I^\beta \rightarrow 2S^\alpha I^-$ $2S^- I^\beta \rightarrow 2S^\beta I^-$	S ³ S ³ -COS	α/β -HSQC- α/β (TROSY-type)	

HCP building blocks

As a starting point, a series of existing and new preparation periods based on HCP and specifically designed to generate particular heteronuclear spin-states suitable for optimum ¹H-to-X coherence transfer are introduced. Figure 2 displays three different 2D HCP-based pulse sequences suitable for COS $2I_z S^- \rightarrow I^-$ coherence transfer, alternatives to the classical HSQC experiment. As similarly described for the INEPT building block (see Equation 10 and Figure 2A), anti-phase S magnetization at the start of the t_1 period can also be achieved by using two related HCP-based preparation periods (see Figures 2B and 2C). The first new proposed HCP preparation building block (see Figure 2B) starts from a 90° (I) pulse applied from the y axis to generate transverse I_x magnetization that is converted to anti-phase $I_y S_z$ magnetization after applying an orthogonal HCP(y) sequence (Equation 5b). Anti-phase S magnetization is created after

two simultaneous 90° (I,S) pulses:

$$I_z \xrightarrow{90_y^I} I_x \xrightarrow{HCP(y)} 2I_y S_z \xrightarrow[90_x^S]{90_x^I} -2I_z S_y. \quad (11)$$

Alternatively, a second very interesting preparation building block (see Figure 2C) that has never reported can be used to generate a similar anti-phase magnetization. The longitudinal I_z magnetization is affected directly by the HCP(y) process as described in Equation 5c to generate multiple-quantum coherences in the form of $I_y S_x$. This perturbation is equivalent to the initial 90° (I)-delay- 90° (S) block usually found in HMQC-type experiments. The resulting MQC can be converted to the desired anti-phase $I_z S_x$ magnetization via a single 90° I(x) pulse:

$$I_z \xrightarrow{HCP(y)} -2I_y S_x \xrightarrow{90_x^I} -2I_z S_x. \quad (12)$$

However, a major inconvenience is that the required time to achieve this anti-phase state in these

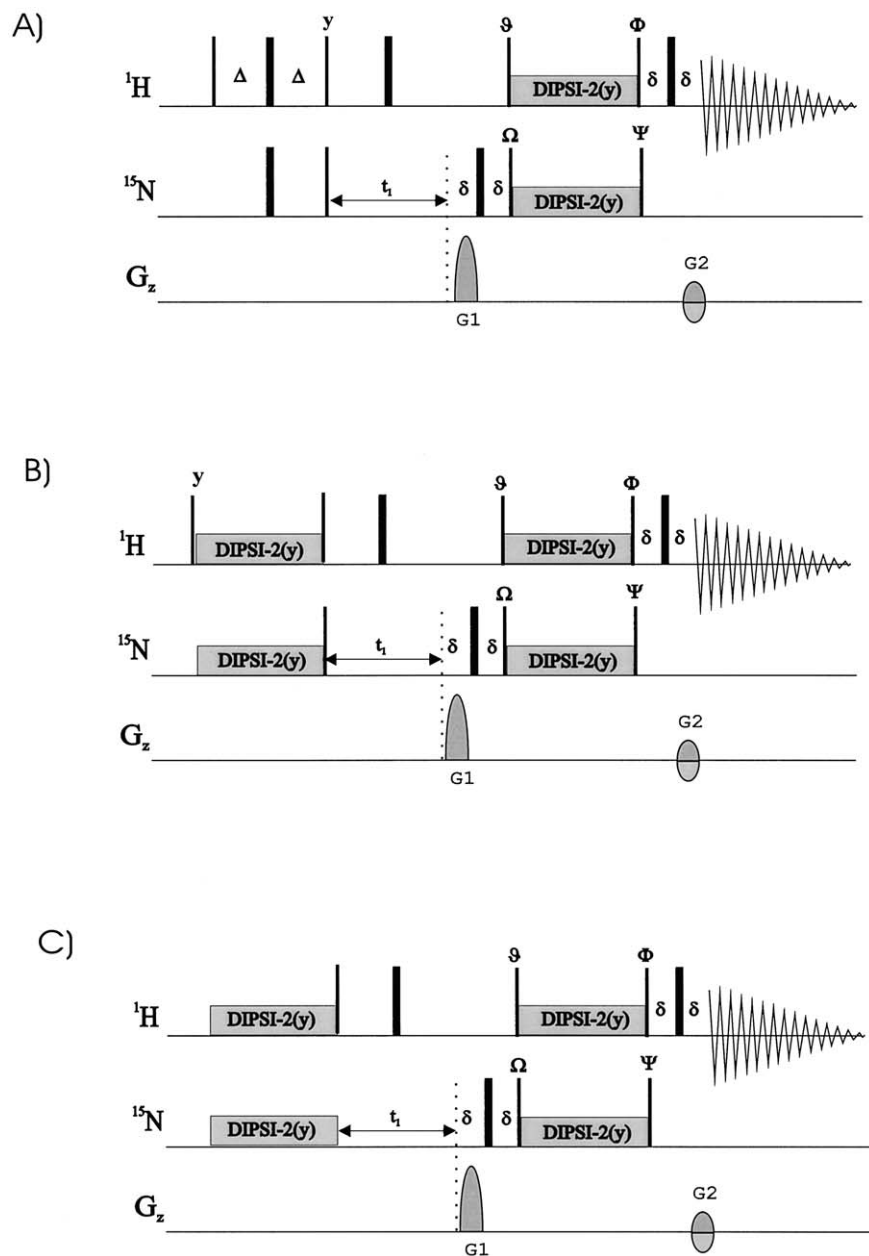


Figure 2. General pulse schemes for the sensitivity-improved gradient-enhanced COS $2I_z S^- \rightarrow I^-$ NMR experiments involving anti-phase S magnetization during the t_1 variable period: (A) 2D INEPT-HCP and B-C) 2D HCP-HCP NMR experiments. Narrow and wide rectangles represent 90° and 180° pulses, respectively, applied from x axis unless otherwise indicated. See text for discussion about the phase Φ , Ω , ϑ and Ψ of 90° pulses embedding the DIPSII-2 sequence. For the HCP mixing process, DIPSII-2 rf fields are simultaneously applied from the y-axis in both channels during a mixing period (τ) usually optimised to $1/J(\text{IS})$. Echo- and anti-echo data are recorded in alternate scans by inverting the G_2 gradient and the phase Ψ or Ω of the corresponding 90° pulse, depending of the used version. Gradients optimised to $(\gamma_I/\gamma_S) : 1$ are also indicated by shaded shapes on the line G_z . In (A) a minimum two-step phase cycle is applied on the first 90° S pulse ($x, -x$) and the receiver ($x, -x$). In (B) and (C) EXORCYCLE is applied to the 180° S pulse ($x, y, -x, -y$) and the receiver ($x, -x$). In F1-coupled HCP experiments, the central 180° ^1H pulse in the middle of the t_1 period is not applied. For labelled bio-molecule samples dissolved in 90% $\text{H}_2\text{O}/10\%$ D_2O several experimental options are feasible. For instance, in the initial INEPT pulse train, a purge gradient during the zz filter combined with water flip-back can improve water suppression. For ^{13}C -labelled proteins, an inversion adiabatic ^{13}C pulse can optionally be placed at the middle of the t_1 period in order to avoid ^{15}N - ^{13}C coupling constant evolution in the F_1 dimension.

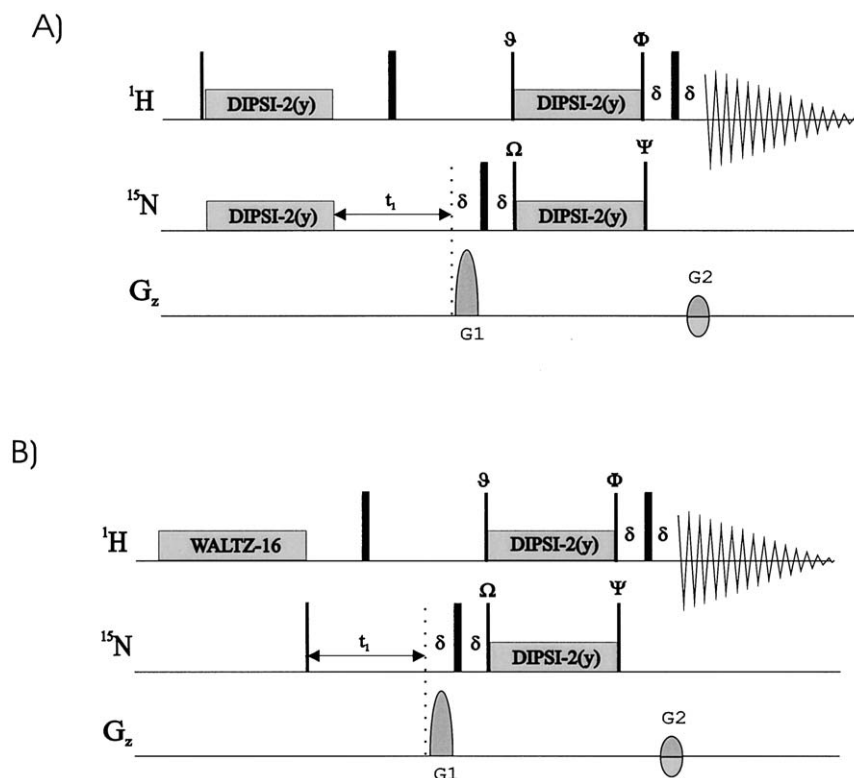


Figure 3. General pulse schemes for the sensitivity-improved gradient-enhanced COS $S^- \rightarrow I^-$ NMR experiments involving in-phase S magnetization during the t_1 variable period: (A) HCP-HCP, and (B) 2D HCP NMR experiments. All other details as described in caption of Figure 2.

HCP building blocks is twice than the classical INEPT pulse train and probably this should be a problem when working on large biomolecules with short transverse relaxation times.

On the other hand, it is also possible to design COS $S^- \rightarrow I^-$ NMR experiments involving in-phase S magnetization during the t_1 period. Some preparation periods widely used are a refocused INEPT building block or a pulse sequence starting directly from a 90° (S) pulse (as shown in Figure 3B). A very effective alternative to achieve this in-phase magnetization should be the implementation of an HCP building block as described from Equation 5a and displayed in Figure 3A.

$$I_z \xrightarrow{90_x^I} -I_y \xrightarrow{HCP(y)} -S_y. \quad (13)$$

The main goal of the present work is the proposal of a universal HCP-based building block as a powerful mixing process in 2D correlation experiments (Figure 1B). It basically consists of an HCP(y) element embedded with 90° I and S pulses each one applied

with a specific ϑ , Ω , Φ , or Ψ phase. As shown in Figures 2 and 3, this HCP mixing process can be combined with any type of preparation period because it has the ability to manipulate both in-phase and anti-phase magnetization in an appropriate way. As another important feature of the proposed HCP mixing process, all sequences presented in Figures 2 and 3 can be also recorded without the central 180° ^1H pulse in the middle of t_1 period. In these cases, the above mentioned in-phase or anti-phase magnetization present at the start of the t_1 period evolves freely under the effect of both chemical shift and heteronuclear coupling constant, giving a mixture of modulated in-phase and anti-phase magnetizations at the end of this t_1 period that can also be manipulated accordingly. It will be shown that this class of NMR experiments afford w1-coupled 2D correlation spectra that combined in a specific way achieve spin-state-selective to spin-state-selective (S^3S^3 -COS: $2I^{\alpha/\beta}S^- \rightarrow 2I^-S^{\alpha/\beta}$) E. COSY-type and TROSY-type coherence transfer.

In principle, the three different HCP-based preparation periods described before could be also combined

with typical INEPT mixing building blocks usually employed in HSQC-type experiments, affording a complete family of HCP-INEPT NMR experiments, but not details will be given here. In addition, as commented before, it should be also possible to design a complete family of HCP experiments involving MQC during the t_1 period in an HMQC-like fashion. The resulting COS $I^-S^- \rightarrow I^-S^{\alpha/\beta}$ NMR experiments could be classified in the same way as described for the INADEQUATE-CR experiment (Nielsen et al., 1995, 1996; Nielsen and Sorensen, 1996; Untidt and Nielsen, 2000; Meissner and Sorensen, 2002) but they neither will be treated here.

INEPT-HCP experiments

The first proposed NMR pulse sequence substitutes the last retro-INEPT building block in the HSQC pulse scheme by the HCP mixing building block, affording the INEPT-HCP experiment depicted in Figure 2A.

Table 2 summarizes five different INEPT-HCP pulse sequences that can be designed with different finalities as a function of which of the four 90° pulses and from which axis (defined as ϑ , Ω , Φ , and Ψ) they are applied. The analysis of such gradient-selected sequences can be easily made taking into account that the anti-phase magnetization just before the HCP mixing process is better described as the sum of two orthogonal cartesian operators:

$$2I_zS^- = 2I_zS_x - 2iI_zS_y. \quad (14)$$

A particular example of this INEPT-HCP experiment was already described (Schleucher et al., 1994; Sattler et al., 1995b) in which the retro-INEPT building block was substituted by a planar heteronuclear TOCSY scheme to achieve *anti-phase to in-phase coherence-order selective*, AI-COS $2I_zS^- \rightarrow I^-$, coherence transfer similarly as described in the popular HSQC-PEP experiment. The planar mixing process was generated by embedding the HCP(y) block into 90° I and S pulses applied from the orthogonal x-axis. Analytical polarization and coherence-transfer behaviour under such planar mixing hamiltonians have been reported (Glaser and Quant, 1996; Krishnan and Rance, 1997; Schedletzky et al., 1998). The echo transfer mechanism (Table 2 – entry a) can be described arising from two initial and independent

anti-phase components:

$$\begin{aligned} 2I_zS^- &= 2I_z(S_x - iS_y) \xrightarrow[90_x^S]{90_x^I} \\ &-2I_yS_x + i2I_yS_z \xrightarrow{HCP(y)} \\ &-I_z - iI_x \xrightarrow{90_x^I} \\ &I_y - iI_x \xrightarrow{\delta-180_x^I-\delta} -I_y - iI_x = -iI^-. \end{aligned} \quad (15)$$

Analysing several combinations of 90° pulses and phases, it is also possible to design four new INEPT-HCP experiments without modify the pulse sequence timing. The first AA-COS (*Anti-phase to Anti-phase coherence-order selective coherence transfer*) pulse scheme incorporates a 90° (S) pulse from the x-axis before the HCP process and a 90° (I) from the x-axis after the HCP process. The resulting magnetization is the sum of two different components and, therefore, sensitivity-enhanced spectra will be obtained (Table 2 – entry b):

$$\begin{aligned} 2I_zS^- &= 2I_z(S_x - iS_y) \xrightarrow{90_x^S} \\ &2I_zS_x - i2I_zS_z \xrightarrow{HCP(y)} \\ &2I_xS_z - i2I_zS_z \xrightarrow{90_x^I} \\ &2I_xS_z + i2I_yS_z \xrightarrow{\delta-180_x^I-\delta} \\ &2I_xS_z - i2I_yS_z = 2I^-S_z. \end{aligned} \quad (16)$$

Similar results are obtained in the second proposed AA-COS pulse sequence, in which the HCP mixing process is embedded between four 90° I and S pulses with the phases specified in Table 2 – entry c:

$$\begin{aligned} 2I_zS^- &= 2I_z(S_x - iS_y) \xrightarrow[90_x^S]{90_y^I} \\ &2I_xS_x - i2I_xS_z \xrightarrow{HCP(y)} \\ &2I_xS_x - i2I_zS_x \xrightarrow[90_y^S]{90_x^I} \\ &-2I_xS_z - i2I_yS_z \xrightarrow{\delta-180_x^I-\delta} \\ &-2I_xS_z + i2I_yS_z = -2I^-S_z. \end{aligned} \quad (17)$$

Otherwise, heteronuclear S^3 states are generated by combining simultaneous in-phase and anti-phase magnetizations. Thus, two related AS³-COS (*Anti-phase to Selective-spin-state coherence-order selective coherence transfer*) pulse schemes can be designed. The first AS³-x-COS approach (the x index

Table 2. Summary of coherence-order transfer pathways in COS $2I_zS^- \rightarrow I^-$ NMR experiments involving antiphase magnetization at the start of t_1 and displayed in Figure 2 as a function of the 90° pulses (and their phases) embedding the HCP process. In the echo/anti-echo procedure, the gradient G2 is inverted with the phase Ω (a–c) or Ψ (d–e)

	Phases of 90° pulses				Coherence-order transfer pathway	Type of transfer mechanism	Equation
	ϑ	Ω	Φ	Ψ			
a)	x	x	x	–	$2I_zS^- \rightarrow I^-$	AI-COS	15
b)	–	x	x	–	$2I_zS^- \rightarrow 2I^-S_z$	AA-COS	16
c)	y	x	x	y	$2I_zS^- \rightarrow 2I^-S_z$	AA-COS	17
d)	x	–	y	x	$2S^-I_z \rightarrow 2S^\alpha I^-$	AS ³ -COS	18
	x	–	y	–x	$2S^-I_z \rightarrow 2S^\beta I^-$		
e)	x	y	–	x	$2S^-I_z \rightarrow 2S^\alpha I^-$	AS ³ -COS	19
	x	y	–	–x	$2S^-I_z \rightarrow 2S^\beta I^-$		

stands for the I_yS_x component before the HCP(y) process) should be defined as (Table 2 – entry d):

$$\begin{aligned}
 2I_zS^- &= 2I_z(S_x - iS_y) \xrightarrow{90_x^I} \\
 -2I_yS_x + i2I_yS_y &\xrightarrow{HCP(y)} -I_z + i2I_yS_y \\
 &\xrightarrow{90_y^I} -I_x \pm i2I_yS_z \xrightarrow{\delta-180_x^I-\delta} \\
 &\xrightarrow{90_{\pm x}^S} -I_x \mp i2I_yS_z = -2I^-S^{\alpha/\beta}
 \end{aligned} \quad (18)$$

and the second AS³-z-COS experiments (Table 2 – entry e):

$$\begin{aligned}
 2I_zS^- &= 2I_z(S_x - iS_y) \xrightarrow{90_x^I} \\
 &\xrightarrow{90_y^S} \\
 2I_yS_z + i2I_yS_y &\xrightarrow{HCP(y)} -I_x + i2I_yS_y \\
 &\xrightarrow{90_{\pm x}^S} -I_x \pm i2I_yS_z \xrightarrow{\delta-180_x^I-\delta} \\
 -I_x \mp i2I_yS_z &= -2I^-S^{\alpha/\beta}.
 \end{aligned} \quad (19)$$

In these AS³-COS experiments, separate spin-edited $2I^-S^\alpha$ and $2I^-S^\beta$ 2D correlation spectra should be obtained by inverting the phase Ψ of the last 90° S pulse. Due to the co-addition of equivalent pathways, both S³ edited experiments also present maximum sensitivity, similarly as predicted for the HSQC- α/β experiment (Sorensen et al., 1997, 1999; Andersson et al., 1998b; Kozminski, 1999).

HCP-HCP experiments

NMR pulse schemes using exclusive HCP processes in both preparation and mixing periods can also be designed, as shown in Figures 2B, 2C and 3A. In fact, the theoretical basis of this type of 2D heteronuclear correlation HCP experiments were discussed some years ago (Ernst et al., 1991) but they did not include the use of pulsed-field gradients for coherence selection. A similar HCP-HCP pulse sequence has also been reported to measure proton exchange rates in proteins (Zangger and Ermitage, 1998).

The general HCP-HCP scheme is suitable to study both COS $2I_zS^- \rightarrow I^-$ and $S^- \rightarrow I^-$ coherence transfers involving anti-phase and in-phase X magnetization, respectively, during the t_1 period as a function of the preparation period. In the case of $2I_zS^- \rightarrow I^-$ type transfer, analogous AI-, AA-, and AS³-COS experiments described for the INEPT-HCP experiment (Figure 2A and Table 2) can be also designed for the two schemes depicted in Figure 2B and 2C (see Equations 11 and 12, respectively) and no more details will be given here on these versions because similar results are obtained as shown in Equations 15–19.

In addition, it is also possible to design several new COS $S^- \rightarrow I^-$ HCP-HCP type experiments using the basic pulse sequence of Figure 3A with the pulses and phases specified in Table 3.

When no 90° pulses are applied embedding the second HCP mixing process, an II-COS (*In-phase to In-phase coherence-order selective*) coherence transfer experiment (Table 3 – entry a) should be obtained but with reduced sensitivity because only one compon-

Table 3. Summary of coherence-order transfer pathways in COS $S^- \rightarrow I^-$ NMR experiments involving in-phase magnetization at the start of t_1 and displayed in Figure 3 as a function of the 90° pulses (and their phases) embedding the HCP process. In the echo/anti-echo procedure, the gradient G2 is inverted with the phase Ψ (b–d)

	Phases of 90° pulses				Coherence-order transfer pathway	Type of transfer mechanism	Equation
	ϑ	Ω	Φ	Ψ			
a)	–	–	–	–	$S^- \rightarrow I^-$	II-COS	20
b)	–	x	x	x	$S^- \rightarrow 2I^- S_z$	IA-COS	21
c)	–	y	–	x	$S^- \rightarrow 2I^- S^\alpha$	IS ³ -COS	22
	–	y	–	–x	$S^- \rightarrow 2I^- S^\beta$		
d)	–	–	y	x	$S^- \rightarrow 2I^- S^\alpha$	IS ³ -COS	23
	–	–	y	–x	$S^- \rightarrow 2I^- S^\beta$		

ent contributes at the observable signal.

$$S^- = S_x - iS_y \xrightarrow{HCP(y)} 2S_y I_z - iI_y \xrightarrow{\delta-180_x^t-\delta} -2S_y I_z + iI_y = \frac{-1}{2} I^- \quad (20)$$

A sensitivity-enhanced IA-COS (*In-phase to Anti-phase coherence-order selective coherence transfer*) experiment resulting of the addition of two equivalent anti-phase magnetizations can be designed (Table 3 – entry b):

$$S^- = S_x - iS_y \xrightarrow{90_x^S} S_x - iS_z \xrightarrow{HCP(y)} 2S_y I_z + i2S_y I_x \xrightarrow{90_x^t} -2S_z I_y + i2S_z I_x \xrightarrow{\delta-180_x^t-\delta} 2S_z I_y + i2S_z I_x = 2iS_z I^- \quad (21)$$

On the other hand, two equivalent S³-edited experiments can also be developed by appropriate arrangement of the 90° pulses. Thus, an IS³-x-COS (*In-phase to Selective-spin-state coherence-order selective coherence transfer* via the S_x component) experiment (Table 3 – entry c)

$$S^- = S_x - iS_y \xrightarrow{HCP(y)} 2S_y I_z - iI_y \xrightarrow{90_y^t} \pm 2S_z I_x - iI_y \xrightarrow{90_{\pm x}^S} \pm 2S_z I_x + iI_y \xrightarrow{\delta-180_x^t-\delta} \pm 2S_z I_x + iI_y = 2I^- S^{\alpha/\beta} \quad (22)$$

and an IS³-z-COS (*In-phase to Selective-spin-state coherence-order selective coherence transfer* via the S_z component) experiment (Table 3 – entry d)

$$S^- = S_x - iS_y \xrightarrow{90_y^S} -S_z - iS_y \xrightarrow{HCP(y)} 2S_y I_x - iI_y \xrightarrow{90_{\pm x}^S} \pm 2S_z I_x - iI_y \xrightarrow{\delta-180_x^t-\delta} \pm 2S_z I_x + iI_y = 2I^- S^{\alpha/\beta} \quad (23)$$

would afford separate α or β -spin-edited 2D correlation spectra, depending of the phase (x or –x) of the last 90° (S) pulse.

Several INEPT-based NMR pulse sequences specifically designed to achieve II-COS transfer have been already described (Sattler et al., 1995a,b; Reiss et al., 2002), but all these experiments started from a 90° (S) pulse, similarly as shown in the proposed HCP scheme of Figure 3B in which all possibilities outlined in Table 3 could be also applied. The major inconvenience of this approach is that the overall sensitivity depends on the $T_1(X)$ and on the effective heteronuclear NOE generated during the relaxation delay. A hypothetical sensitivity-improved II-COS HCP scheme would afford in-phase coherence order selective $S^- \rightarrow I^-$ coherence transfer via an isotropic HCP mixing process but not experimental details was given (Sattler et al., 1995a). This type of ¹H-X HCP experiments have been found interest in correlation and relaxation NMR experiments applied on ³¹P in nucleic acids (Kellog, 1992; Kellog et al., 1992; Kellog and Schweitzer, 1993; Wang et al., 1994; Schweitzer et al.,

1996) and on ^{113}Cd in metalloproteins (Gardner and Coleman, 1994; Schweitzer et al., 1996). The proposed COS HCP pulse sequences outlined here could be found interest in NMR applications requiring in-phase X magnetization in some stage, as found, for instance, in the measurement of T_1 , T_2 , and $T_{1\text{ro}}$ ^{15}N relaxation times and heteronuclear ^1H - ^{15}N NOEs in proteins.

F1-coupled HCP experiments

As a very promising feature of the HCP strategy, it is possible to remove the 180° (^1H) pulse at the center of the variable evolution t_1 period in all pulse sequences depicted in Figures 2 and 3 to allow the free evolution of heteronuclear coupling constants simultaneously to X chemical shift evolution. For instance, in all F1-coupled experiments of Figure 2 starting from anti-phase magnetization, a mixture of in-phase and anti-phase magnetization should be obtained at the end of the t_1 period and just before the mixing HCP process as follows:

$$\begin{aligned} 2I_z S_y &\xrightarrow{t_1} 2I_z S_y \cos(\Omega t_1) \cos(\pi J t_1) \\ &- S_x \cos(\Omega t_1) \sin(\pi J t_1) \\ &- 2I_z S_x \sin(\Omega t_1) \cos(\pi J t_1) \\ &- S_y \sin(\Omega t_1) \sin(\pi J t_1). \end{aligned} \quad (24)$$

In a closely analogous way, the 180° (I) pulse in pulse sequences involving in-phase magnetization at the start of the t_1 period (Figure 3) can be also omitted affording a similar mixture of in-phase and anti-phase magnetization:

$$\begin{aligned} -S_y &\xrightarrow{t_1} -S_y \cos(\Omega t_1) \cos(\pi J t_1) \\ &+ 2I_z S_x \cos(\Omega t_1) \sin(\pi J t_1) \\ &+ S_x \sin(\Omega t_1) \cos(\pi J t_1) \\ &+ 2I_z S_y \sin(\Omega t_1) \sin(\pi J t_1). \end{aligned} \quad (25)$$

In both cases, the resulting transverse S magnetization can be treated as the sum of two different coherences, $2(I^\alpha + I^\beta)S^-$. Omitting signs and normalization factors, each one of this four terms can be converted to observable proton magnetization combining the universal HCP mixing schemes of Figure 1B with the pulses and phases specified in Table 4, and without any other extra modification of the original pulse sequences. This feature allows the development of many different versions of *spin-state-selective to*

spin-state-selective coherence-order-selective ($\text{S}^3\text{S}^3\text{-COS: } 2I^{\alpha/\beta}S^- \rightarrow 2I^-S^{\alpha/\beta}$) coherence transfer experiments in two different ways. If the HCP(y) sequence is embedded between four 90° pulses applied from the x axis (Table 4 – entry a), the following conversion is established:

$$\begin{array}{ccc} \text{Term - I : } 2I_z S_y & & 2I_y S_z \\ \text{Term - II : } S_x & \xrightarrow{90_x^I} & S_x \\ \text{Term - III : } 2I_z S_x & \xrightarrow{90_x^S} & 2I_y S_x \\ \text{Term - IV : } S_y & & S_z \\ & & (26) \\ \xrightarrow{\text{HCP(y)}} & \begin{array}{ccc} I_x & & I_x \\ 2I_z S_y & \xrightarrow{90_x^I} & 2I_y S_z \\ I_z & \xrightarrow{90_x^S} & I_y \\ 2I_x S_y & & 2I_x S_z. \end{array} \end{array}$$

From Equation 8, it can be deduced that the initial terms (I+II) in this Equation 26 represent $2I^\alpha S^-$ whereas the terms (III+IV) represent $2I^\beta S^-$ at the end of t_1 period. Thus, when echo and anti-echo data are recorded by simultaneous inversion of the G2 gradient and the first 90° (S) pulse, two simultaneous and independent $\text{S}^3\text{-S}^3\text{ COS } 2I^\alpha S^- \rightarrow 2I^-S^\alpha$ and $2I^\beta S^- \rightarrow 2I^-S^\beta$ transfers are accomplished after appropriate echo/anti-echo processing, in which connected transitions are exclusively transferred in an in-phase E. COSY manner. The experiment recorded with $\Psi = -x$ would give the anti-diagonal $2I^\alpha S^- \rightarrow 2I^-S^\beta$ and $2I^\beta S^- \rightarrow 2I^-S^\alpha$ transfer mechanism whereas the spectrum generated from sequence 3a acquired under the same conditions (entry a from Table 4) would show an anti-phase E. COSY coupling pattern.

On the other hand, it is also possible to transfer spin-state-selective to single-transition states in a TROSY-like way, by means of two different HCP mixing sequences. The first approach should be (Table 4 – entry b)

$$\begin{array}{ccc} \text{Term - I : } 2I_z S_y & & 2I_y S_y \\ \text{Term - II : } S_x & \xrightarrow{90_x^I} & S_z \\ \text{Term - III : } 2I_z S_x & \xrightarrow{90_x^S} & 2I_y S_z \\ \text{Term - IV : } S_y & & S_y \\ & & (27) \\ \xrightarrow{\text{HCP(y)}} & \begin{array}{ccc} 2I_y S_y & & 2I_y S_z \\ 2I_x S_y & \xrightarrow{90_x^S} & 2I_x S_z \\ I_x & & I_x \\ I_y & & I_y \end{array} \end{array}$$

and the second (Table 4 – entry c):

Table 4. Summary of coherence-order transfer pathways in COS $2I^{\alpha/\beta}S^- \rightarrow 2I^-S^{\alpha/\beta}$ E. COSY and TROSY HCP-based NMR pulse sequences displayed in Figures 2–3 (without the 180° pulse in the middle of t_1 period) as a function of the 90° pulses (and their phases) embedding the HCP process. In the echo/anti-echo procedure, the gradient G2 is inverted with the phase Ω (a–b) or Ψ/ϑ (c)

	Phases of 90° pulses				Coherence-order transfer pathway	Type of transfer mechanism	Equation
	ϑ	Ω	Φ	Ψ			
a)	x	x	x	x	$2S^-I^\alpha \rightarrow 2S^\alpha I^-$ & $2S^-I^\beta \rightarrow 2S^\beta I^-$	S^3S^3 -COS	26
	x	x	x	-x	$2S^-I^\alpha \rightarrow 2S^\beta I^-$ & $2S^-I^\beta \rightarrow 2S^\alpha I^-$		
b)	x	y	-	x	$2S^-I^\alpha \rightarrow 2S^\alpha I^-$	S^3S^3 -COS	27
	x	y	-	-x	$2S^-I^\alpha \rightarrow 2S^\beta I^-$		
	-x	y	-	x	$2S^-I^\beta \rightarrow 2S^\alpha I^-$		
	-x	y	-	-x	$2S^-I^\beta \rightarrow 2S^\beta I^-$		
c)	x	-	y	x	$2S^-I^\alpha \rightarrow 2S^\alpha I^-$	S^3S^3 -COS	28
	x	-	y	-x	$2S^-I^\alpha \rightarrow 2S^\beta I^-$		
	-x	-	y	x	$2S^-I^\beta \rightarrow 2S^\alpha I^-$		
	-x	-	y	-x	$2S^-I^\beta \rightarrow 2S^\beta I^-$		

$$\begin{array}{l}
 \text{Term - I : } I_z S_y \\
 \text{Term - II : } S_x \\
 \text{Term - III : } I_z S_x \\
 \text{Term - IV : } S_y
 \end{array}
 \xrightarrow{90_x^I}
 \begin{array}{l}
 I_y S_y \\
 S_x \\
 I_y S_x \\
 S_y
 \end{array}
 \quad (28)$$

$$\begin{array}{l}
 I_y S_y \\
 I_z S_y \\
 I_z \\
 I_y
 \end{array}
 \xrightarrow{HCP(y)}
 \begin{array}{l}
 I_y S_z \\
 I_x S_z \\
 I_x \\
 I_y
 \end{array}
 \xrightarrow{90_y^I}
 \begin{array}{l}
 I_y S_z \\
 I_x S_z \\
 I_x \\
 I_y
 \end{array}
 \xrightarrow{90_x^S}
 \begin{array}{l}
 I_x S_z \\
 I_x \\
 I_x \\
 I_y
 \end{array}$$

In contrast to the generated E. COSY pattern described by Equation 26, these analogous TROSY transfers can be understood as two simultaneous and independent *spin-state-selective to anti-phase coherence-order-selective* (S^3A -COS) $2I^\alpha S^- \rightarrow 2I^-S$ (terms I+II) and *spin-state-selective to in-phase coherence-order-selective* (S^3I -COS) $2I^\beta S^- \rightarrow I^-$ (terms III+IV) mechanism transfers. In practice, the addition of all coherence pathways described in Equations 27 and 28 afford exclusive single-transition coherence transfer mechanisms, in which four different subspectra ($2I^\alpha S^- \rightarrow 2I^-S^\alpha$, $2I^\alpha S^- \rightarrow 2I^-S^\beta$, $2I^\beta S^- \rightarrow 2I^-S^\alpha$, and $2I^\beta S^- \rightarrow 2I^-S^\beta$) can be generated by different combination of the phases Ψ (x or -x) and ϑ (x or -x). Experimentally that means that only one of the four peaks of an IS spin system is obtained, providing interesting alternatives to classical TROSY experiments.

In summary, taking the five pulse sequences depicted in Figures 2 and 3 and the three different options summarized in Table 4, it has been proposed up to five

versions to perform E. COSY-like experiments and ten different variants to run TROSY-like experiments using the proposed HCP mixing process.

Experimental part

Because NH spin systems resonate in narrow and very specific spectral regions in both 1H and ^{15}N spectra, all proposed HCP experiments are highly suitable to be applied to natural abundance peptides and also ^{15}N -labeled proteins. We have chosen a small natural-abundance model tri-peptide sample showing four NH resonances in the conventional 1H spectrum. Gradient selection affords clean spectra at natural abundance with perfect suppression of the large 1H - ^{14}N magnetization. Figure 4 shows several F2-coupled 2D HCP-HCP spectra recorded with the AI-COS, AA-COS, and AS 3 -COS versions of the sequence depicted in Figure 3A and with the pulses and phases proposed in Table 3.

Figure 5 shows several F1,F2-coupled 2D HCP-HCP spectra using the pulse sequence of Figure 3A and recorded with the different S^3 - S^3 COS approaches specified in Table 4. All possible coupling pattern topologies are clearly visible. Analogous F1,F2-coupled 2D experiments recorded with sequences of Figures 2 and 3 give similar results and data is therefore not shown.

Figure 6 shows some the most relevant 1D traces taken from specific 2D spectra displayed in Figures 4–5. As predicted theoretically, sensitivity-enhancement

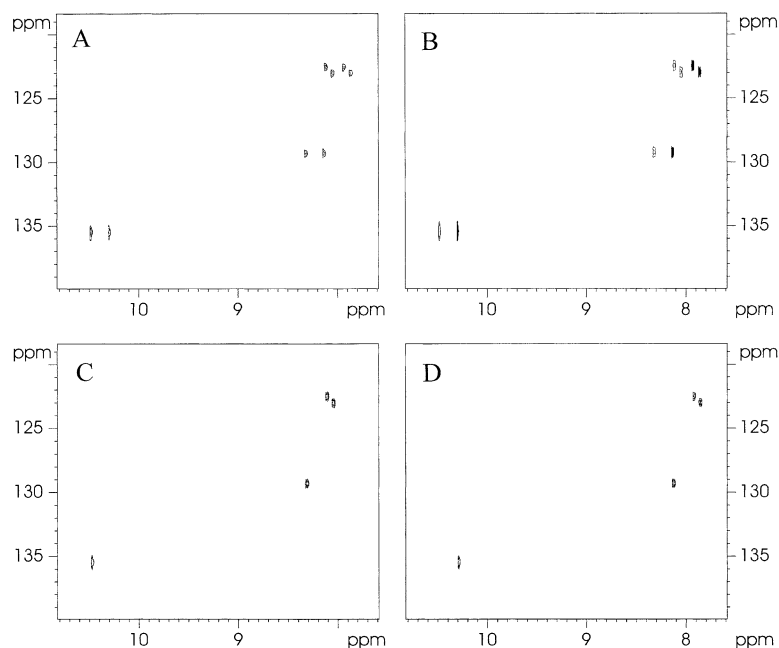


Figure 4. 2D ^1H - ^{15}N HCP based spectra of a 50 mg of the tripeptide N-succinyl-Ala-Ala-Ala-p-nitroanilide, **1**, sample dissolved in 0.7 ml. of DMSO- d_6 , acquired with the pulse sequence of Figure 3A, using different combination of pulses and phases specified in Table 3: (A) No 90° pulses are applied (see entry a); (B) The 90° pulses specified with Φ , Ω and Ψ phases are all applied from the x axis (see entry b); (C–D) Only the 90° pulses specified with Ω and Ψ phases are applied from (C) the y and x axis, and (D) the y and $-x$ axis, respectively (see entry c). All spectra were recorded in a AVANCE 500 spectrometer equipped with a 5 mm inverse broadband probehead incorporating Z-gradients. HCP was achieved by applying simultaneous 5.5 KHz DIPSI-2 pulse trains of duration 11 ms in both ^1H and ^{15}N channels, and centered to the corresponding NH regions (8 and 120 ppm, respectively). Four scans of 1024 complex points were collected for each of the 64 t_1 increments. A recovery delay of 1 sec was used prior to each scan and the total acquisition time for each of the 2D spectra was 8 minutes. 2D data were processed with a 90° shifted sine bell window in both F1 and F2 dimensions followed by Fourier transformation. The t_1 interferograms were zero-filled and linear predicted prior to multiplication with the window function and transformed with 1024×1024 complex points. Sine-shaped gradients of duration (δ) of 1 ms were followed by a recovery time of 100 μs and optimised to a 80:8.1 ratio.

is preserved in all spectra. As a reference, the in-phase multiplet obtained from an INEPT-HCP experiment using a planar TOCSY mixing sequence (Figure 2A combined with phases and pulses defined in the entry a of Table 2) is shown (Figure 6A). Among minimal experimental imperfections, the sensitivity of anti-phase (Figure 6B), S^3 -edited (Figures 6C–D), E, COSY (Figure 6E) and TROSY (Figure 6F) cross peaks shown the same ratios for this small molecule.

One important point to see is how effective is the HCP mixing process over the typical spectral range found in peptides and proteins. Figure 7 shows the experimental signal intensity of NH resonances as a function of ^{15}N frequency offset in an AS^3 -COS HCP-HCP experiment. It can be seen that a 5.5 KHz DIPSI-2 sequence is enough uniform in intensity, phase and, very importantly, there is no considerable cross talk from the other spin-state in a enough range of frequencies (80–150 ppm). For large biomolecules, strong rf power must be avoided for the HCP processes in or-

der do not heat the sample. Of course, the design of improved HCP sequences requiring less rf power for a given effective bandwidth will be of great importance.

To check the successful application of the proposed HCP pulse sequences on more drastic conditions, they have been also applied on a ^{13}C , ^{15}N -doubly labelled 64-residues protein dissolved in 90% H_2O -10% D_2O . In all cases, perfect solvent suppression without need of presaturation of other solvent-suppression building blocks for all in-phase, anti-phase and S^3 HCP experiments was also achieved as described before (data not shown). As an example, Figure 8 shows two AS^3 -COS 2D ^1H - ^{15}N HCP-HCP spectra of this protein. In order to compare the overall sensitivity of these spectra with conventional HSQC experiments, Figure 9 shows some 1D rows extracted from different 2D spectra in which experimental sensitivity ratios are as expected theoretically. When compared to equivalent HSQC- α/β spectra, similar ratios are obtained and clean S^3 excitation is achieved without presence of residual

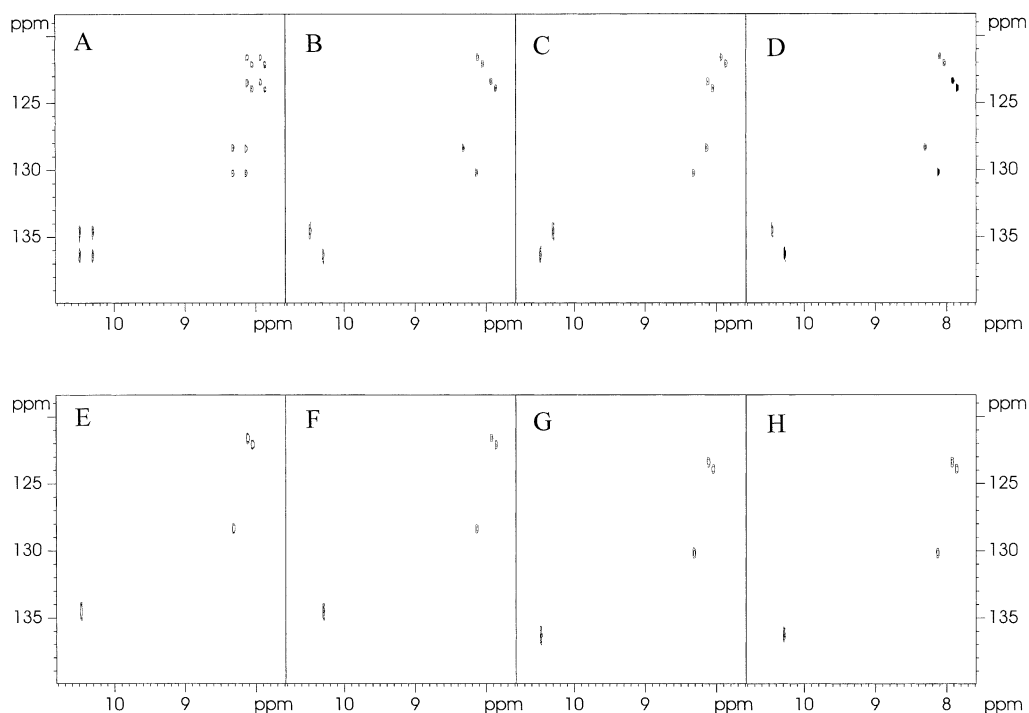


Figure 5. 2D F1-coupled ^1H - ^{15}N HCP-based spectra of **1**, acquired with the pulse sequence of Figure 3A without the 180° ^1H pulse applied in the middle of t_1 and using different combination of pulses and phases. (A) Conventional F1,F2-coupled HCP spectra recorded with any 90° pulse as described in Table 3 – entry a; (B–C) E. COSY spectra obtained from the pulse sequence of Figure 2B with the two combinations described in Table 4, entry a; (D) same as B but using the sequence of Figure 3A. In this case the E. COSY spectrum shows an anti-phase pattern; (E–H) TROSY spectra obtained with the four combinations described in Table 4, entry b. Other experimental conditions as described in caption of Figure 4.

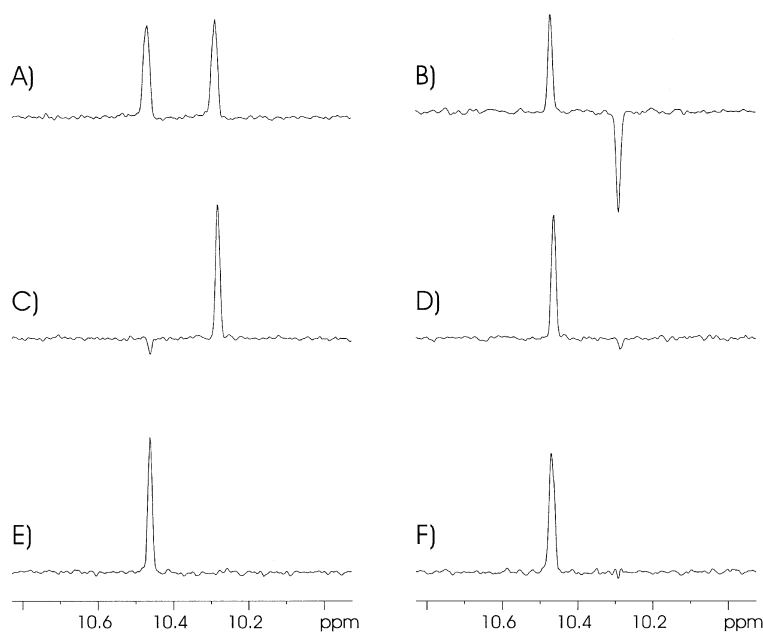


Figure 6. Comparison of the relative sensitivity of selected 1D F2 traces taken at 134.8 ppm from the spectra displayed in the following HCP experiments: (A) F2-coupled in-phase (Figure 4A), (B) F2-coupled anti-phase (Figure 4B), (C) F2- α -edited (Figure 4C), (D) F2- β -edited (Figure 4D), (E) E. COSY (Figure 5B), and (F) TROSY (Figure 5E), respectively.

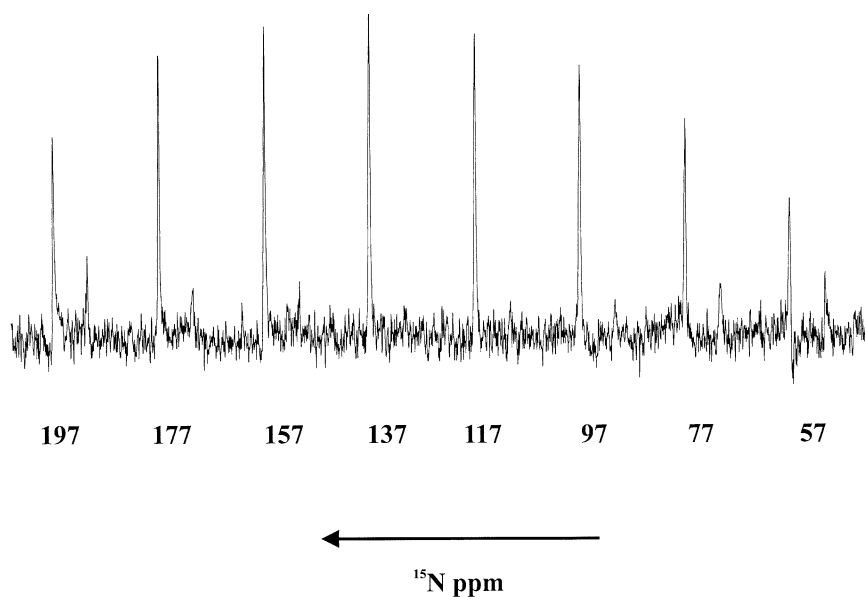


Figure 7. Experimental dependence of signal intensity versus ^{15}N offset in the HCP-HCP experiment recorded in the same experimental conditions as described in Figure 4C. Eight 1D spectra were recorded by converting the sequence of Figure 3A to 1D by removing the variable evolution delay ($t_1 = 0$) and using an offset increment of 20 ppm. Two cycles of a 5.5 KHz DIPSI-2 pulse scheme was used as a HCP mixing sequence (90° ^{15}N pulse of 45 μs). All spectra were processed with a line broadening of 1 Hz.

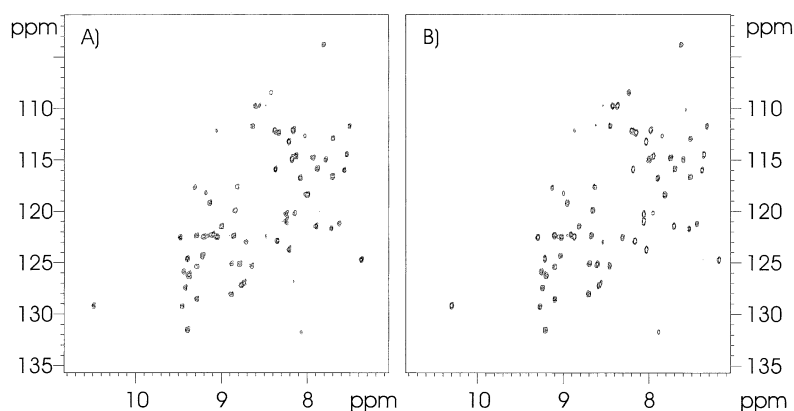


Figure 8. 2D F2-spin-edited HCP-HCP spectra of a 1 mM 64 residues doubly-labeled protein acquired with the pulse sequence of Figure 3A and the pulses and phases specified in Table 3 – entry d. Thirteen-two scans of 1024 complex points were collected for each of the 256 t_1 increments. A recovery delay of 1 sec was used prior to each scan and the total acquisition time for each of the 2D spectra was 90 minutes. Other experimental details as described in Figure 4.

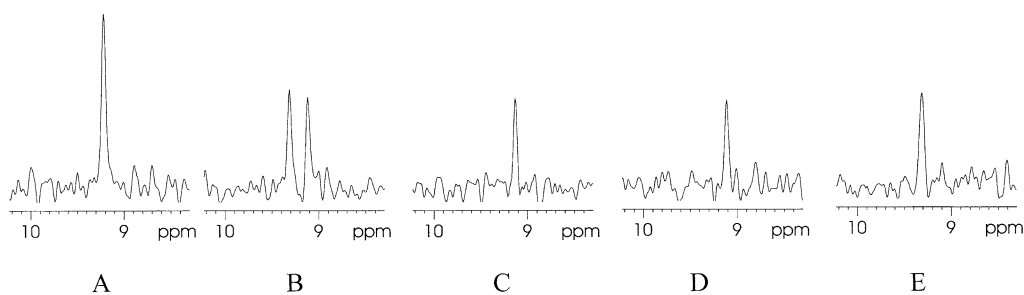


Figure 9. Comparison of selected 1D row traces of different 2D correlation experiments recorded under the same experimental conditions specified in Figure 8. (A) Conventional F2-decoupled HSQC-PEP; (B) Conventional F2-coupled HSQC-PEP; (C) S^3 -edited HSQC- α experiment; (D, E) α and β S^3 -edited HCP-HCP experiment as described in Figure 8.

cross talk, confirming the feasibility of HCP as an alternative to HSQC experiments. Some approaches to compensate the presence of unwanted relaxation-induced cross talk have been proposed in HSQC-type experiments (Meissner et al., 1998b; Schulte-Herbrüggen and Sorensen, 2000; Schulte-Herbrüggen et al., 2001) and therefore it should be interesting to consider this effect in HCP experiments when different sizes of $^1J(\text{NH})$ are present as, for instance, in the measurement of residual dipolar couplings in anisotropic media. Although the proposed methodology has been successfully applied to a small peptide and to a moderate protein in a 500 MHz spectrometer, the impact of these methodologies on larger proteins in higher magnetic fields must be evaluated and compared to the existing NMR experiments

Conclusions

It has been demonstrated that sensitivity-enhanced HCP-based correlation experiments can be used for many several purposes by proper setting of the 90° pulses embedding the HCP mixing process. Several methods that combine in-phase, anti-phase or spin-state-selective multiplet pattern with two-dimensional heteronuclear shift correlation experiment have been proposed, without altering the overall timing of the pulse sequence and, therefore, minimizing undesired relaxation effects. In particular, the new suggested S^3 edited experiments can be interesting for the measurement of scalar and dipolar coupling constants and also for structural and dynamic NMR studies using specific TROSY-related applications. In principle, all the described coherence-transfer equations could be also applicable to other broadband HCP sequences (Schwendinger et al., 1994; Glaser and Quant, 1996; Luy and Glaser, 2000) and, therefore, the design and optimisation of new ultra-broadband heteronuclear cross-polarization sequences using improved multiple-pulse sequences or adiabatic pulses promise the use of HCP-based methodologies as attractive alternatives to the most popular HSQC pulse trains. In addition, the different HCP elements presented here can be incorporated as effective preparation and mixing building blocks in multidimensional NMR experiments. Much work on the practicalities of these proposed HCP experiments and their application on large biomolecules in high magnetic fields are in progress.

Acknowledgements

This research has been financed by the MCYT of Spain through Project BQU2003-01677. All NMR experiments were performed at the Servei de Resonància Magnètica Nuclear of the Universitat Autònoma de Barcelona. I am indebted to Prof S.J. Glaser and Dr W. Bermel for their helpful comments and discussions.

References

- Andersson, P., Annala, A. and Otting, G. (1998a) *J. Magn. Reson.*, **133**, 364–367.
- Andersson, P., Weigelt, J. and Otting, G. (1998b) *J. Biomol. NMR*, **12**, 435–441.
- Bertrand, R.D., Monitz, W.B., Garroway, A.N. and Chingas, G.C. (1978) *J. Am. Chem. Soc.*, **100**, 5227–5229.
- Bodenhausen, G. and Ruben, D.J. (1980) *Chem. Phys. Lett.* **69**, 185–189.
- Chingas, G.C., Garroway, A.N., Bertrand, R.D. and Monitz, W.B. (1981) *J. Chem. Phys.*, **74**, 127–156.
- Czisch, M. and Boelens, R. (1998) *J. Magn. Reson.*, **134**, 158–160.
- Ernst, M., Griesinger, C., Ernst, R.R. and Bermel, W. (1991) *Mol. Phys.* **74**, 219–252.
- Gardner, K.H. and Coleman, J.E. (1994) *J. Biomol. NMR*, **4**, 761–774.
- Glaser, S. and Quant, J.J. (1996) In *Advances in Magnetic and Optical Resonance*, Vol. 19, Warren, W.S. (Ed.), Academic Press, pp. 59–251.
- Griesinger, C., Sorensen, O.W. and Ernst, R.R. (1985) *J. Am. Chem. Soc.*, **107**, 6394–6395.
- Hartmann, S.R. and Hahn, E.L. (1962) *Phys. Rev.* **128**, 2042–2053.
- Kay, L.E., Keifer, P. and Saarinen, T. (1992) *J. Am. Chem. Soc.*, **114**, 10663–10665.
- Kellog, G.W. (1992) *J. Magn. Reson.* **98**, 176–182.
- Kellog, G.W. and Schweitzer, B.I. (1993), *J. Biomol. NMR*, **3**, 577–595.
- Kellog, G.W., Szewczak, A.A., and Moore, P.B. (1992) *J. Am. Chem. Soc.*, **114**, 2727–2728.
- Kozmiski, W. (1999) *J. Magn. Reson.*, **137**, 408–412.
- Krishnan, V.V. and Rance, M. (1995), *J. Magn. Reson. A*, **116**, 97–106.
- Krishnan, V.V. and Rance, M. (1997), *J. Magn. Reson. A*, **124**, 205–209.
- Levitt, M.H. (1991) *J. Chem. Phys.* **94**, 30–38.
- Luy, B. and Glaser, S.J. (2000) *J. Magn. Reson.* **142**, 369–371.
- Majumdar, A. and Zuiderweg, E.R.P. (1995) *J. Magn. Reson. A*, **113**, 19–31.
- Meissner, A. and Sorensen, O.W. (2002) *Conc. Magn. Reson.*, **14**, 141–154.
- Meissner, A., Duss, J.O. and Sorensen, O.W. (1997) *J. Biomol. NMR*, **10**, 89–94.
- Meissner, A., Schulte-Herbrüggen, T., Briand, J. and Sorensen, O.W. (1998a) *Mol. Phys.*, **95**, 1137–1142.
- Meissner, A., Schulte-Herbrüggen, T. and Sorensen, O.W. (1998b) *J. Am. Chem. Soc.*, **120**, 7989–7990.
- Muller, L. and Ernst, R.R. (1979) *Mol. Phys.*, **38**, 963
- Nielsen, N.C., Thogersen, H. and Sorensen O.W. (1995) *J. Am. Chem. Soc.*, **117**, 11365–11366.
- Nielsen, N.C., Thogersen, H., and Sorensen, O.W. (1996) *J. Chem. Phys.*, **105**, 3962–3968.

- Ottiger, M., Delaglio, F. and Bax, A. (1998) *J. Magn. Reson.*, **131**, 373–378.
- Palmer III, A.G., Cavanagh, J., Wright, P.E. and Rance, M. (1991) *J. Magn. Reson.*, **93**, 151–170.
- Pervushin, K., Riek, R., Wider, G. and Wüthrich, K. (1997) *Proc. Natl. Acad. Sci.*, **94**, 12366–12371.
- Reiss, T.O., Khaneja, N. and Glaser, S.J. (2002) *J. Magn. Reson.*, **154**, 192–195.
- Richardson, J.M., Clowes, R.T., Boucher, W., Domaille, P.J., Hardman, C.H., Keeler, J. and Laue, E.D. (1993) *J. Magn. Reson. B*, **101**, 223–227.
- Sattler, M., Schleucher, J., Schedletsky, O., Glaser, S.J., Griesinger, C., Nielsen, N.C. and Sorensen, O.W. (1996) *J. Magn. Reson. A*, **119**, 171–179.
- Sattler, M., Schwendinger, M., Schleucher, J., and Griesinger, C. (1995a) *J. Biomol. NMR*, **6**, 11–22.
- Sattler, M., Schmidt, P., Schleucher, J., Schedletsky, O., Glaser, S.J. and Griesinger, C. (1995b) *J. Magn. Reson. B*, **108**, 235–242.
- Schedletsky, O., Luy, B. and Glaser, S.J. (1998) *J. Magn. Reson.*, **130**, 27–32.
- Schleucher, J., Sattler, M. and Griesinger, C. (1993) *Angew. Chem. Int. Ed. Engl.*, **32**, 1489–1491.
- Schleucher, J., Schwendinger, M., Sattler, M., Schmidt, P., Schedletsky, O., Glaser, S.J., Sorensen, O.W. and Griesinger, C. (1994) *J. Biomol. NMR*, **4**, 301–306.
- Schulte-Herbrüggen, T. and Sorensen, O.W. (2000) *J. Magn. Reson.*, **144**, 123–128.
- Schulte-Herbrüggen, T., Untidt, T.S., Nielsen, N.C. and Sorensen, O.W. (2001) *J. Chem. Phys.*, **115**, 8506–8514.
- Schweitzer, B.I., Gardner, K.H. and Tucker-Kellog, G. (1999) *J. Biomol. NMR*, **6**, 180–188.
- Schwendinger, M.G., Quant, J.J., Schleucher, J., Glaser, S.J. and Griesinger, C. (1994) *J. Magn. Reson. A*, **111**, 115–120.
- Shirakawa, M., Walchli, M., Shimizu, M. and Kyogoku, Y. (1995) *J. Biomol. NMR*, **5**, 323–326.
- Simorre, J.P., Zimmermann, G.R., Pardi, A., Farmer II, B.T. and Mueller, L. (1995) *J. Biomol. NMR*, **6**, 427–432.
- Sklenar, V., Dieckmann, T., Butcher, S.E. and Feigon, J. (1996) *J. Biomol. NMR*, **7**, 83–87.
- Sorensen, M.D., Meissner, A. and Sorensen, O.W. (1997) *J. Biomol. NMR*, **10**, 181–186.
- Sorensen, M.D., Meissner, A. and Sorensen, O.W. (1999) *J. Magn. Reson.*, **137**, 237–242.
- Sorensen, O.W., Eich, G.W., Levitt, M.H. and Bodenhausen, G. (1983) *Prog. Nucl. Magn. Reson. Spectrosc.*, **21**, 503–569.
- Untidt, T.S. and Nielsen, N.C. (2000) *J. Chem. Phys.*, **113**, 8464–8471.
- Untidt, T.S., Schulte-Herbrüggen, T., Luy, B., Glaser, S.J., Griesinger, C., Sorensen, O.W. and Nielsen, N.C. (1998) *Mol. Phys.*, **95**, 787–796.
- Untidt, T.S., Schulte-Herbrüggen, T., Sorensen, O.W. and Nielsen, N.C. (1999) *J. Phys. Chem. A*, **103**, 8921–8926.
- Wang, H. and Zuiderweg, E.R.P. (1995) *J. Biomol. NMR*, **5**, 207–211.
- Wang, K.Y., Goljer, I. and Bolton, P.H. (1994) *J. Magn. Reson. B*, **103**, 192–196.
- Wijmenga, S.S., Heus, H.A., Leeuw, H.A.E., Hoppe, H., Van der Graaf, M. and Hilbers, C.W. (1995) *J. Biomol. NMR*, **5**, 82–86.
- Zangger, K. and Armitage, I.M. (1998) *J. Magn. Reson.*, **135**, 70–75.
- Zuiderweg, E.R.P. (1990) *J. Magn. Reson.*, **89**, 533–542.
- Zuiderweg, E.R.P., Zeng, L., Brutscher, B. and Morshauer, R.C. (1996) *J. Biomol. NMR*, **8**, 147–160.